PULSED BEAM CURRENT MONITOR WITH A TOROIDAL COIL

Hideki Dewa, Yoshihisa Iwashita, Hirokazu Fujita, Masanori Ikegami,
Makoto Inoue, Shigeru Kakigi, Masaki Kando, Akira Noda,
Hiromi Okamoto, and Toshiyuki Shirai
Institute for Chemical Research, Kyoto University
Gokanosho, Uji-city, Kyoto-fu 611, Japan

Abstract

We developed a pulsed beam current monitor. This current monitor can measure the 50 μs macro pulsed beam from the proton linac. The available current range is from 30 μA to 10 mA. This monitor is toroidal coil type, and the pulsed current can be measured without beam destruction. We developed the special circuit for the I-V converter whose input impedance is almost zero. The time constant of the droop was 35 ms, that is much longer than the beam pulse width of 50 μs, and the droop was negligibly small.

Introduction

The measurement of the pulsed beam current by the toroidal coil has a disadvantage of the droop of the output signal. The finite inductance of the coil and non-zero input impedance of the I-V converter cause this droop. The pulse width of our ICR proton linac is around 50 μs, and the minimum peak current to be measured is the order of 100 μA. For the measurement by the oscilloscope, the conversion gain must be greater than 1000 V/A, and the time constant of the droop must be longer than 1 ms.

When a resister is a converter, the value must be carefully determined. Higher resistance is needed for a high output voltage, and the lower resistance is needed for the less droop. Then a new converter circuit was developed for the compatibility of the low input impedance and high gain.

Measurement Principle

When the charged particle passed through a toroidal core, secondary current I_2 is induced and given by

$$I_2(t) = \frac{I_1}{n}\exp(-\frac{Z}{L}t) \qquad (1)$$

where I_1, n and Z are the pulsed beam current, the number of the turns of the secondary winding, the input impedance of the I-V converter, respectively. The inductance of the coil L is given by

$$L = A_L \times n^2, \qquad (2)$$

where A_L is constant of the core and is proportional to the magnetic permeability.

Because the time constant of the droop is L/Z, the L must be large and Z must be small for the long droop time. For this purpose, larger n is desirable, but the secondary current become low. When a resister is used as the I-V converter, the low resistor is desirable for the long droop time, but not suitable for the high gain. Therefore, the long droop time and high gain are not compatible. For example if the droop time is 1 ms and the gain is 10 and A_L is 14000 nH/n^2, n must be 714 and R must be 7140 Ω. It seems impossible to wind so many turns of wires on the small core.

Then we developed the converter circuit so that we can get both merit. The circuit diagram is shown in Fig 1. This circuit is an application circuit of the negative impedance converter (NIC). The ratio of the input current I_2 and the inverse current I_3 is given by

$$\frac{I_2}{I_3} = \frac{R_3}{R_2}. \qquad (3)$$

The input impedance of the converter is given by

$$Z = \frac{R_1R_3 - R_2R_4}{R_3} \qquad (4)$$

Therefore , when the following relation is satisfied;

$$R_1R_3 = R_2R_4, \qquad (5)$$

the input impedance become zero, and the time constant of the droop become theoretically infinity. Because the output voltage is $-R_1I_2$, the conversion gain is $-R_1$.

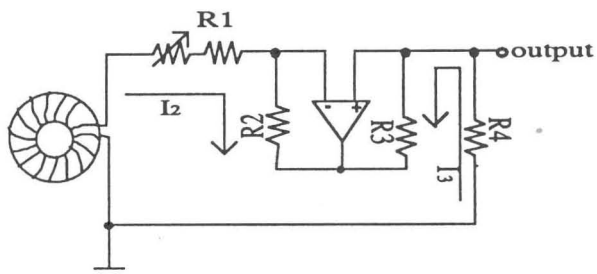

Fig.1 Circuit diagram of the I-V converter with NIC

Toroidal Coil

The toroidal coil is shown in Photo 1. The core of the coil is made of Mn-Zn ferrite, which is TDK H5C2 T28×13×16. The relative magnetic permeability of the core is 10000, the inner and outer diameters are 13 mm and 28 mm, respectively, and the width is 16 mm. The A_L of the core is 14000 nH/n^2, and the number of the turns is 30. The measured inductance of the coil is 14.0 mH. And another one turn coil was winded for the calibration.

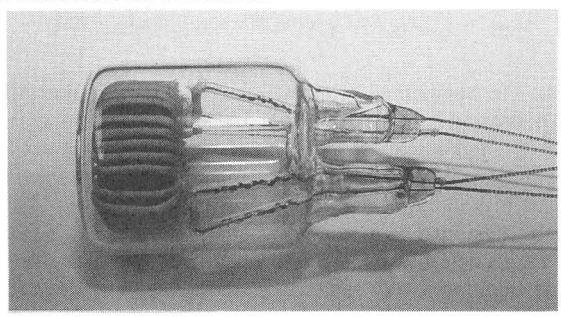

Photo 1 Toroidal coil

Considering the easiness of the production and the vacuum isolation, it is sealed in a glass container whose inner and outer diameter is 12 mm and 40 mm respectively. The secondary winding is a copper wire coated by a formal resin. The diameter of the wire is 0.5 mm, which is covered with a glass fiber tube for insulation considering a hot environment in the sealing process.

Circuit System

The detailed circuit diagram of the designed I-V converter is shown in Fig. 2. To keep the equation (5), precision metal-film resistors are used in these four resistors R_1 - R_4, and R_1 is composed of a metal-film resistor and a 10 Ω variable resistor. The variable resistor should be adjusted to near the 5 Ω as the droop of the wave form is decreased. Because the resistor R_3 is low, the large output current increases the power dissipation and raises its temperature. Therefore a current booster circuit is attached at the output of the operational amplifier, that can decrease the thermal drift.

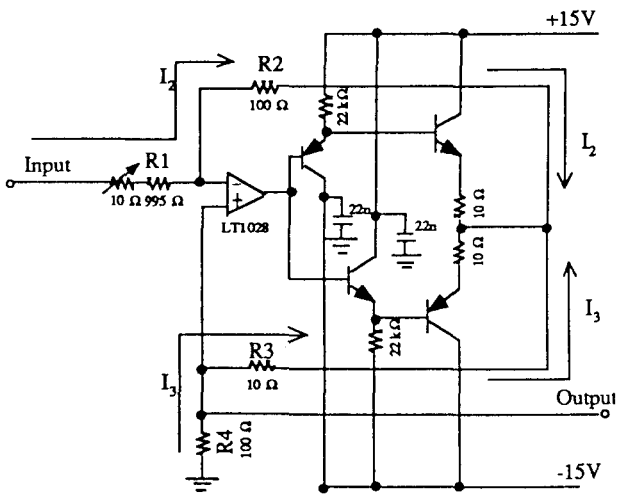

Fig.2 Detailed circuit diagram of the I-V converter

The secondary current from the toroidal coil goes through the coaxial cable and feed through, to the I-V converter. Because the number of turns of the coil is 30 and we want the total conversion gain to be 1000 V/A, the gain of another second stage amplifier is decided as 30. Then the output signal goes to the offset canceling circuit in the control room that is located out of the accelerator room, and the processed signal is measured by the oscilloscope.

When the coil is installed in the beam matching section between the RFQ linac and the Alvarez linac which keep high power RF of 433 MHz in them, even small fraction of the power leak can be picked up by the coil. To eliminate the RF contamination, a low pass filter with 200 MHz cutoff is inserted between the coil and the converter. The low pass filter was directly connected to the BNC feed through and the convertor, so that the distance between the coil and the converter could be as short as possible.

There are two reasons that cause the offset of the output signal. One is the thermal drift of the operational amplifier, and the other is the hum from the commercial power line (60 Hz). The thermal drift.was reduced by decreasing the power supply voltage of the operational amplifier of the I-V converter and adding the current booster It was not easy to suppress the hum noise. Because the I-V converter is also sensitive to the low frequency signal, the level of the hum is comparable to the real beam signal at the small beam current. Although the aluminum thin foil is wrapped around the glass container as the electric shield, it is not effective to such low frequency noise.

The glass container of the coil was enclosed by a permalloy sheet for the magnetic shield. That can reduce the hum noise, and the fluctuation of the offset level become low. To keep the offset level at zero, we added the offset canceling circuit after the converter. This circuit holds the output level of the converter just before the pulse signal, and subtracts this level from the original pulse signal. The timing of the sample hold is given by the timing generator of the accelerator system and the delay circuit.

Performance Test With The Function Generator

The current monitor was tested with a test pulse current from a function generator. The test pulse was fed to the primary winding of one turn. The test pulse signal and the output of the second amplifier is shown in Fig.3. The input impedance of the converter should be adjusted to almost zero by the variable resistor so that the droop of the pulse shape decreases. The output pulse shape before and after the adjustment are shown in (a) and (b), respectively. The time constant of the droop is measured as 35 ms when the variable resistor is adjusted well. Thus the droop in the 50 μs is evaluated to be 0.2 %.

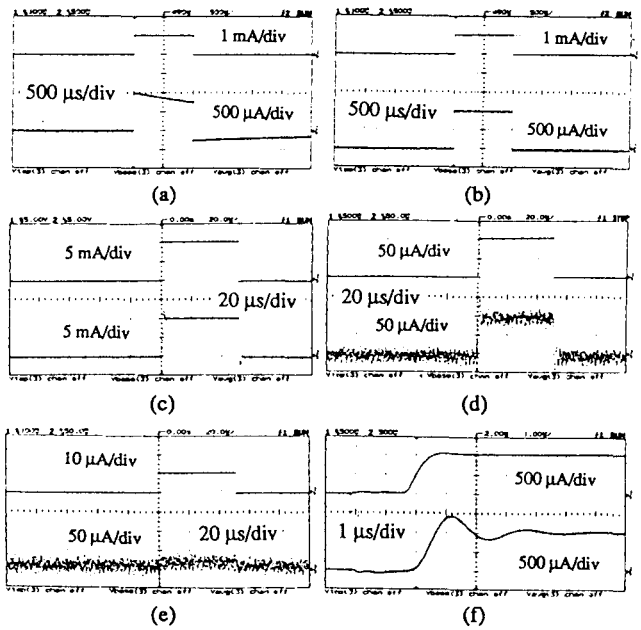

Fig.3 Measurement of the test current. Top signals are test current from the function generator. Bottom signals are output of the current monitor. (a) for not adjusted variable resister R1, (b) for adjusted R1, (c) for 10 mA of primary current, (d) for 100 μA of primary current, (e) for low current test, (f) for the measurement of the rise time.

The output signals at the primary currents of 10 mA and 100 μA are shown in (c) and (d), respectively. We could measure the test pulsed current without the droop. The result when the primary current is 10 μA is shown in (e). Because the noise level of about 30 mV is higher than the signal of 10 mV, the pulse shape is not clear. Thus the minimum current that can be measured is about 30 μA. When the primary current was 1 mA, the rise time of the pulse was 1 μs as shown in (f). This rise time is enough for the measurement of our proton beam.

Beam Test 1

We measured the beam current through the core monitor and that from the faraday cup in the setup shown in Fig.4. This measurement is for the calibration of the beam current monitor by the real beam. Electron suppressor was attached to two points so that the secondary electron emission does not affect the beam current measurement. And the ϕ6 collimator was set in front of the core monitor to prevent that the beams bumped on the core monitor. The result is shown in Photo 2. The signal of the core monitor is almost same as that of faraday cup except the noises. The peak current through the core monitor is 110 μA, and the current of faraday cup was 120 μA. Because there is 5% gain loss in the core monitor circuit, this result was reasonable.

The pedestal offset before and after the beam pulse is the holding offset of the sample hold circuit. The high frequency noise before and after the beam signals are the thyratron noises of the PFN for the klystron power supply.

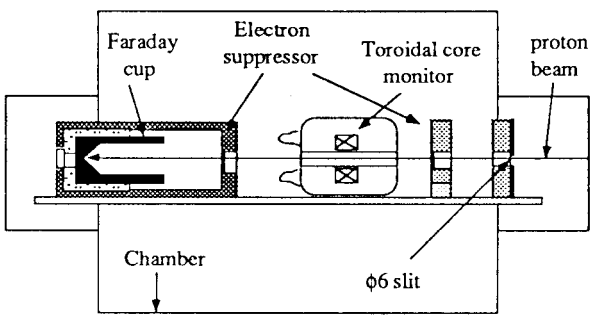

Fig.4 Configuration of the calibration test.

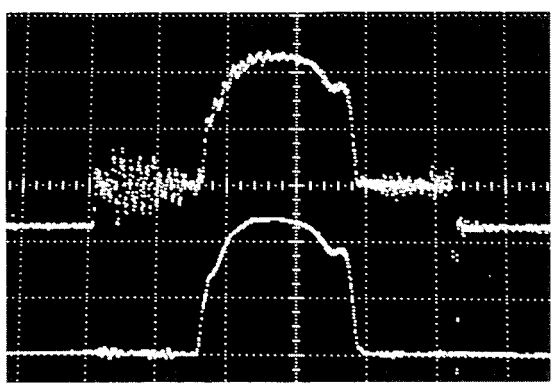

Photo 2 Result of beam calibration test. Top signal from the core monitor, bottom signal from the faraday cup.

Beam Test 2

We measured the beam current after the RFQ linac and before the Alvarez linac. The measured beam current is shown in the photo 3. Two dips were observed just before and after the beam pulse in the top signal. Because these dips were not observed by the second monitor, this signal may be the induced electrons from the RFQ. The measured peak current was 250 μA with the pulse width of about 50 μs. Because the time constant of the droop is much longer than the pulse width, the droop is not seen in the measured pulse shape. The rise time of the pulsed beam was measured to be 4 μs without any rise time corruption caused by the monitoring system.

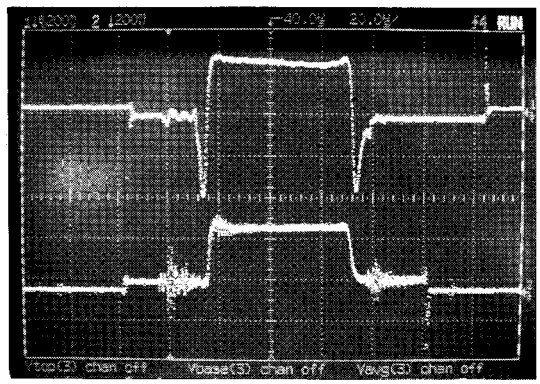

Photo 3 Beam current measured in the beam matching section. After the RFQ in the top, and before the Alvarez in the bottom.

Conclusion

We developed a beam current monitor of the current transformer type. The adjustable input impedance of the I-V converter enables the beam current measurement of the long pulse and low current. The offset canceling circuit made the fluctuation of the offset zero. The frequency range of the monitor is from 30 Hz to 1 MHz, and the wide range current response from 30 μA to 10 mA was realized.

In the beam test, the pulsed beam at 250 μA and with the pulse width of 50 μA was measured without droop and rise time corruption. And the hum noise was much reduced by the offset canceling circuit.

Reference

1) Ryuji Yamada, "New Magnetic Pickup Prove for Charged Particle Beams", Japan. J. Appl. Phys., **1**, (2) 92-100 (1962).
2) John M. Anderson, "Wide Frequency Range Current Transformers", Rev. Sci. Inst., **42**, (7) 915-926 (1971).
3) F.R. Gallegos, L.J. Morrison, and A.A. Browman, "The Development of a Current Monitor System for Measuring Pulsed-Beam Current Over a Wide Dynamic Range", IEEE Trans. Nucl. Sci., **NS-32**, (5) 1959-1961 (1985).
4) R.L. Witkover, E. Zitvogel and V. Castillo, "Beam Current Monitoring in the AGS Booster and its Transfer Lines", Proc. of the 1991 IEEE Particle Accelerator Conf., pp. 1267-1269.
5) L. P. Huelsman, "Theory and Design of Active RC Circuits", McGraw-Hill Inc., New York, (1968).
6) J.G. Graeme, G.E. Tobey, L.P. Huelsman, "Operational Amplifier Design and Applications", Burr-Broun Corporation, (1971).